Improved ferroelectric properties in multiferroic $BiFeO_3$ thin films through La and Nb codoping

Zhenxiang Cheng, Xiaolin Wang, and Shixue Dou
Institute for Superconducting and Electronics Materials, University of Wollongong, New South Wales 2522, Australia

Hideo Kimura and Kiyoshi Ozawa
National Institute for Materials Science, Sengen 1-2-1, Tsukuba, Ibaraki 305-0047, Japan

(Received 30 November 2007; revised manuscript received 6 January 2008; published 4 March 2008)

We report the significant improvement of the ferroelectric properties of $BiFeO_3$ thin film through control of electrical leakage by Nb doping. A very large remanent electrical polarization value of 80 $\mu C/cm^2$ was observed in $Bi_{0.8}La_{0.2}Nb_{0.01}Fe_{0.99}O_3$ thin film on $Pt/Ti/SiO_2/Si$ substrate. The doping effect of Nb in reducing the movable charge density due to oxygen vacancies in $BiFeO_3$ was confirmed by the dielectric measurements. A very small loss was observed in the Nb and La codoped $BiFeO_3$ thin film. As well as the improvement in the ferroelectric properties, the magnetic moment was also enhanced due to the doping of La.

DOI: 10.1103/PhysRevB.77.092101 PACS number(s): 77.80.−e, 77.90.+k

Multiferroic [magnetoelectric (ME)] materials have simultaneous ferroelectric and magnetic orders, which enable the coupling interaction between ferroelectric and magnetic orders.[1,2] This coupling interaction, also named the ME effect, produces various possibilities in the realization of mutual control and detection of electrical polarization and magnetism. As a potential candidate for practical application among the limited choices provided by single phase multiferroic materials, $BiFeO_3$ has attracted enormous attention, due to its multiferroic properties at room temperature (T_C = 1103 K, T_N=643 K).[3–5] However, $BiFeO_3$ is antiferromagnetic, with a *G*-type spin configuration along the $[111]_c$ or $[001]_h$ directions in its pseudocubic or rhombohedral structures, with a superimposed incommensurate cycloid spin structure, which has a periodicity of 620 Å along its $[110]_h$ axis at room temperature, canceling out the macroscopic magnetization.[6,7] However, the long-range ordering of the cycloid spin periodical structure can be broken in thin films, and therefore, the macroscopic magnetic moment can be enhanced.[8] Besides the required large magnetic moment, strong ferroelectric performance is also required for $BiFeO_3$ to be used in either magnetoelectric devices or ferroelectric memory chips. Unfortunately, $BiFeO_3$ has poor ferroelectric performance due to severe electric leakage both in thin films and in bulks. It is believed that the electrical leakage is caused by oxygen vacancies and iron ions with different valences via the formation of shallow energy centers.[9,10] Doping in $BiFeO_3$ has been proved to be effective in suppressing the cycloid structure and enhancing the magnetic moment; for example, La substitution for Bi can improve the magnetic moment in $BiFeO_3$ polycrystalline bulks.[11] The ferroelectric properties, however, were not investigated for these doped samples. Because of the difficulty in controlling oxygen vacancies and the volatility of bismuth, the $BiFeO_3$ film performance depends critically on the deposition methods and conditions.[12–15] The reported electrical polarization values vary significantly from group to group and are inconsistent with each other. It is highly desirable to develop an effective approach by which the current leakage can be significantly reduced, and, in turn, the ferroelectric performance of $BiFeO_3$ thin film will be improved.

In this Brief Report, La doped and La and Nb codoped $BiFeO_3$ thin films on $Pt/Ti/SiO_2/Si$ substrate were fabricated. It was found that the ferroelectric properties in La and Nb codoped $BiFeO_3$ thin films were significantly improved by the doping, and the ferromagnetic moment remains at a high level.

The thin film samples in this work were deposited using a pulsed laser deposition system. Third harmonic generation of a Nd doped yttrium aluminum garnet laser with a wavelength of 355 nm and a repetition rate of 10 Hz was used as the laser source. The targets, having compositions of $Bi_{1-x}La_xNb_yFe_{1-y}O_3$ (x=0,0.1,0.2; y=0,0.01) with 10% excess bismuth, were synthesized by a standard solid-state reaction. The starting chemicals were Bi_2O_3, La_2O_3, Fe_3O_4, and Nb_2O_5, with all supplied by Aldrich at a purity of 99.9%. The thin films were initially deposited on $Pt/Ti/SiO_2/Si$ substrate at 550 °C, then cooled down to room temperature following rapid thermal processing. During the deposition, the dynamic oxygen flow pressure was kept at 20 mTorr.

The phase and structure of the as-deposited films were determined by x-ray diffraction (XRD) using Cu $K\alpha$ radiation on a JEOL 3500 XRD machine. Pt upper electrodes with an area of 0.0314 mm^2 were deposited by magnetron sputtering through a metal shadow mask. The thickness of the films was measured by an optical reflection method with a Filmtek™ 4000 system from Scientific Computing International, USA. Results show that all the thin films studied here have a thickness of around 600 nm. The ferroelectric properties were measured at room temperature by an aixACCT Easy Check 300 ferroelectric tester. Magnetic properties of the thin film samples were investigated on a Quantum Design magnetic property measurement system.

Figure 1 shows the x-ray diffraction patterns of the as-deposited thin films. The undoped $BiFeO_3$ film on $Pt/Ti/SiO_2/Si$ substrate shows a rhombohedral structure with space group *R*3*c*, in apparent contrast to the previous report of a tetragonal *P*4*mm* structure for $BiFeO_3$ polycrystalline thin film on the same substrate.[13] This is based on the character of the single (012) peak at around 22° and the splitting of the (104) and (110) peaks around 32°. $Bi_{0.9}La_{0.1}FeO_3$ maintains a rhombohedral structure, which is manifested by the splitting of the (006) and (202) peaks

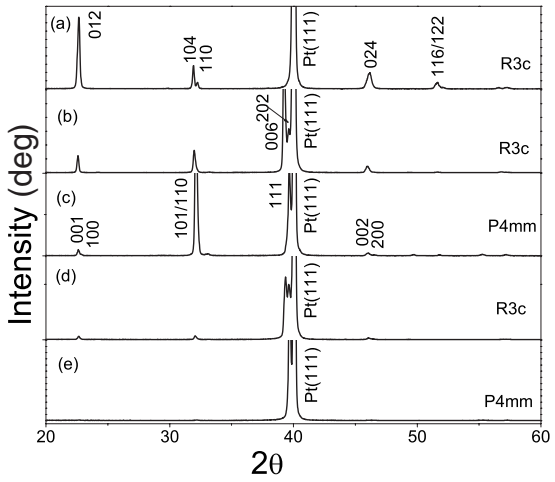

FIG. 1. XRD patterns of the pure, La doped and La and Nb codoped $BiFeO_3$ films on $Pt/Ti/SiO_2/Si$ substrate: (a) $BiFeO_3$, (b) $Bi_{0.9}La_{0.1}FeO_3$, (c) $La_{0.2}Bi_{0.8}FeO_3$, (d) $Bi_{0.9}La_{0.1}Nb_{0.01}Fe_{0.99}O_3$, and (e) $Bi_{0.8}La_{0.2}Nb_{0.01}Fe_{0.99}O_3$. The space groups of these thin films are indicated in the figures. The diffraction peaks are indexed according to their structures.

around 40°. However, $Bi_{0.8}La_{0.2}FeO_3$ thin film shows a tetragonal structure, according to the splitting of the (001) and (100) peaks around 22° and the single (111) peak around 40°. The doping of a tiny amount of Nb into La doped $BiFeO_3$ does not change its structure; therefore, $Bi_{0.9}La_{0.1}Fe_{0.99}Nb_{0.01}O_3$ thin film and $Bi_{0.8}La_{0.2}Fe_{0.99}Nb_{0.01}O_3$ thin film have the rhombohedral structure and the tetragonal structure, respectively. The La doped $BiFeO_3$ thin films show an evolution of the structure that shows a similar trend to that of their bulks. Nevertheless, pure and 10% La doped, including Nb codoped, $BiFeO_3$ thin films do not show such strong rhombohedral distortion as their bulk materials, so that a tendency toward tetragonal symmetry is apparent. Besides the differences observed above, the texture habits of these thin films on $Pt/Ti/SiO_2/Si$ substrate are quite different. Undoped $BiFeO_3$ shows strong epitaxial growth along the $[012]_h$ direction, while the other films prefer to grow along the $[001]_h$ direction for rhombhedral symmetry or the $[111]_t$ direction for tetragonal symmetry, except for the 20% La doped $BiFeO_3$, which shows more preferred growth along its $[101]_t/[110]_t$ direction than its $[111]_t$ direction.

Figure 2 shows the ferroelectric polarization hysteresis loops (P-E loops) of doped and undoped $BiFeO_3$ thin film capacitors. The undoped $BiFeO_3$ has a sensing margin, $2P_r$ $(P_r^+ - P_r^-)$, of 135 $\mu C/cm^2$ at an applied electrical field with a maximum value of 547 kV/cm. Note that freely movable charges appear to contribute significantly to the electrical hysteresis loop, as manifested by the rounded features of the loops, which means that the electrical leakage is severe in these thin films. The remnant polarization of 10% La doped $BiFeO_3$ thin film has a $2P_r$ value of 137 $\mu C/cm^2$ at the breakdown voltage, which is not much improved in comparison to the pure $BiFeO_3$. Yet, the contribution to the polarization from the freely movable charges is reduced, as evidenced by the less rounded features of the loops. The

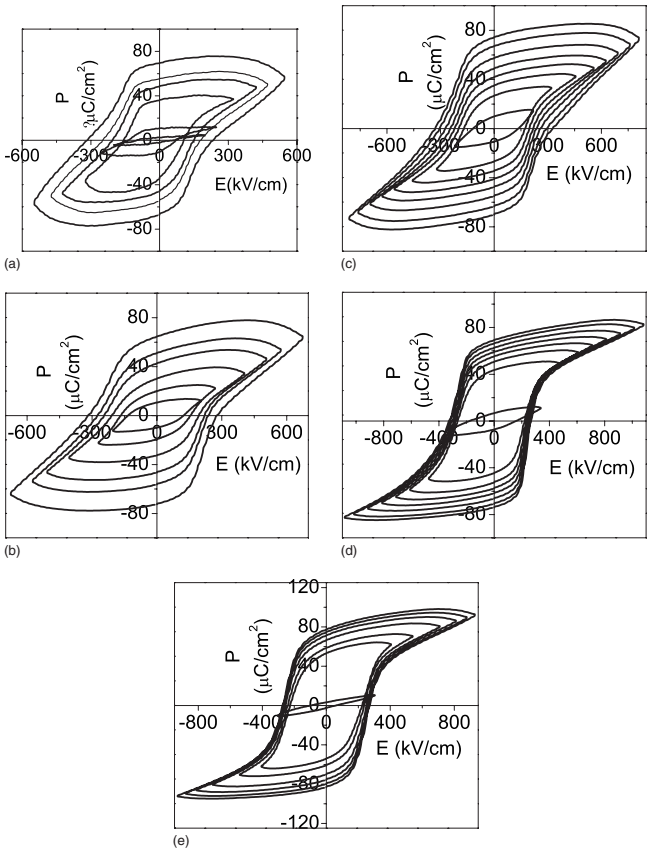

FIG. 2. Ferroelectric polarization loops (P-E loops) of doped $BiFeO_3$ thin film capacitors on $Pt/Ti/SiO_2/Si$ substrate: (a) $BiFeO_3$, (b) $Bi_{0.9}La_{0.1}FeO_3$, (c) $La_{0.2}Bi_{0.8}FeO_3$, (d) $Bi_{0.9}La_{0.1}Nb_{0.01}Fe_{0.99}O_3$, and (e) $Bi_{0.8}La_{0.2}Nb_{0.01}Fe_{0.99}O_3$. All the measurements are at a frequency of 100 Hz and room temperature. Significant improvement of the electric polarization due to reduction in the density of the freely moving charges was observed.

contribution to the polarization from the freely movable charges is further reduced in 1% Nb doped $Bi_{0.9}La_{0.1}FeO_3$ thin film, and a $2P_r$ value of 142 $\mu C/cm^2$ is observed. In comparison with the pure and 10% doped $BiFeO_3$, no rounded features were present; that is, there was no contribution from the freely movable charges in the P-E loops of 20% La doped $BiFeO_3$ thin film. Simultaneously, the value of $2P_r$ was enhanced up to 145 $\mu C/cm^2$. Addition of 1% Nb in 20% doped $BiFeO_3$ further increased the remnant polarization $2P_r$ value up to 160 $\mu C/cm^2$. At the same time, a well developed P-E loop was observed without any observable features pointing to electrical leakage. Another phenomenon observed from the comparison of the P-E loops is that the breakdown voltage was significantly increased by La and Nb codoping.

The La doping into $BiFeO_3$ stabilizes the formation of $BiFeO_3$ phase and reduces the formation of iron rich phases, for example, $Bi_2Fe_4O_9$, which has been proved by XRD results on the bulk materials.[11,16] The formation of the iron rich phase will thus change the ratio of the elements in the thin film and lead to the production of oxygen vacancies and iron ions with different valences. Oxygen vacancies are one of the main sources of movable charges in $BiFeO_3$. Ions with vary-

ing valences will also cause increased conductance, for example, possibly through a possible double exchange mechanism via Fe^{2+}-O-Fe^{3+} chains. Therefore, the movable charges are significantly reduced by doping with La. Nb doping further reduces the movable charge density in La doped $BiFeO_3$. It is believed that the mechanism by which Nb doping works is similar to that for La doping, through reduction of oxygen vacancies by a charge neutralization effect due to the higher valence of Nb (+5) than Fe.

A precise comparison of the enhancement of electrical polarization in $BiFeO_3$ by La doping and codoping of La and Nb is difficult, due to the breaking down of $BiFeO_3$ and 10% La doped $BiFeO_3$ thin films before they are fully switched, but enhancement is observed in the fully switched thin films. It is proposed here that the observed enhancement in remanent polarization is mainly due to doped thin films being more insulating, but enhancement from further structural distortion caused by the doping effect cannot be simply ruled out. Nevertheless, the contribution from this should not be large. This is based on a recent observation of a large polarization of about 60 $\mu C/cm^2$ in $BiFeO_3$ single crystal, which is very close to the value observed in tetragonally distorted $BiFeO_3$ thin film. This is in contrast to the very small polarization observed in pure $BiFeO_3$ in the early work, proving that tetragonal distortation may not be necessary for large electrical polarization.[5,13,17] Another contribution to the observed enhancement in the polarization in the thin film samples is the preferred expitaxial growth direction. It is known that the polarization direction in rhombohedrally or tetragonally distorted $BiFeO_3$ is along its $[001]_h$ or perovskite pseudocubic $[111]_c$ direction. Undoped $BiFeO_3$ thin films on $Pt/Ti/SiO_2/Si$ substrate prefer to grow along the rhombohedral $[012]_h$ direction, which involves great deviation from the polarization maximum direction of $[001]_h$. For the 10% La doped $BiFeO_3$ thin films, including the 1% Nb codoped sample, the preferred growth direction is $[001]_h$, which is the polarization maximum direction. Similarly, 20% La doped samples, especially the Nb and 20% La codoped one, show preferred growth along the $[111]_c$ direction, which is the polarization maximum direction. The preferred growth

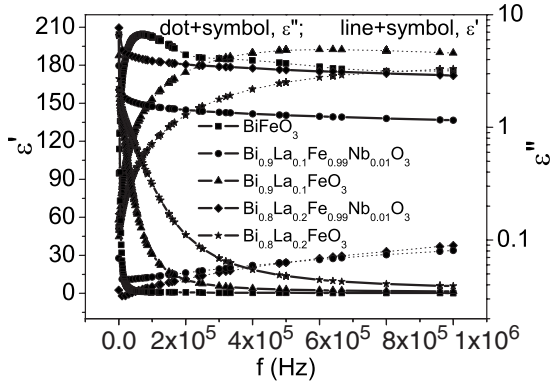

FIG. 3. Frequency dependence from 100 Hz to 1 MHz of the real part and imaginary part of the dielectric permittivity of undoped and doped $Pt/BiFeO_3/Pt$ thin film capacitors measured at room temperature. Dotted line+symbol is for ε''; solid line +symbol is for ε'.

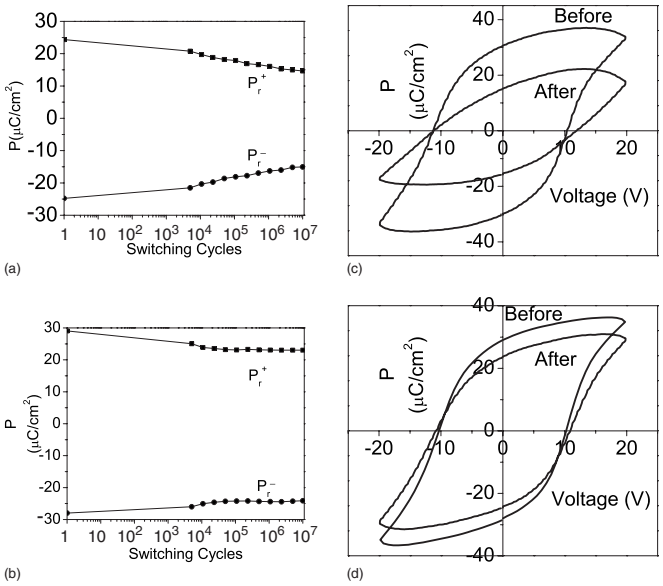

FIG. 4. Comparison of fatigue measurements of the (a) $Bi_{0.9}La_{0.1}FeO_3$ and (b) $Bi_{0.9}La_{0.1}Nb_{0.01}Fe_{0.99}O_3$ thin film samples. The *P-E* loops before fatigue testing and after the test are also plotted, (c) $Bi_{0.9}La_{0.1}FeO_3$ and (d) $Bi_{0.9}La_{0.1}Nb_{0.01}Fe_{0.99}O_3$. The polarization measurement is at 20 V, the switching voltage is 12 V, and the frequency is 5 kHz.

along the polarization maximum direction in doped and codoped samples will directly contribute to the observed polarization enhancement.

Frequency dependence of the real part and the imaginary part of the dielectric permittivity of the doped and undoped thin film capacitors was measured at room temperature (as shown in Fig. 3). The real parts of the dielectric permittivity are 184, 148, 86, 31, and 1.4 at 100 kHz for the samples with compositions of $Bi_{0.8}La_{0.2}Nb_{0.01}Fe_{0.99}O_3$, $Bi_{0.9}La_{0.1}Nb_{0.01}Fe_{0.99}O_3$, $Bi_{0.8}La_{0.2}FeO_3$, $Bi_{0.9}La_{0.1}FeO_3$, and $BiFeO_3$, respectively. Apparent differences in the dielectric permittivity due to the doping are obvious. Similarly, the dielectric loss is significantly reduced with La and Nb codoping. The ε'' values of the $Bi_{0.8}La_{0.2}Nb_{0.01}Fe_{0.99}O_3$, $Bi_{0.9}La_{0.1}Nb_{0.01}Fe_{0.99}O_3$, $Bi_{0.8}La_{0.2}FeO_3$, $Bi_{0.9}La_{0.1}FeO_3$, and $BiFeO_3$ films are 0.038, 0.047, 0.69, 1.78, and 6.47 at 100 kHz at room temperature, respectively. Apparently, the five samples can be divided into two groups. One group includes three samples, the solely La doped and undoped $BiFeO_3$ films, while the other group includes the two Nb and La codoped samples. In contrast to the large loss and small ε' shown by the non-Nb doped samples, the Nb doped samples have large ε' and small loss. This indicates that Nb doping drastically reduced the free movable charge density in the $BiFeO_3$ thin film, while no La doping contribution in reducing the density of the freely movable charges in $BiFeO_3$ is apparent. This observation is in accordance with the results from the electrical polarization measurements; that is, due to the significant reduction in the movable charge density, Nb doped $BiFeO_3$ thin films show perfectly saturated *P-E* loops.

Fatigue measurements of the doped $BiFeO_3$ thin film capacitors are shown in Fig. 4. A 10% La doped $BiFeO_3$ thin film does not show much improvement in fatigue resistance

in comparison to the undoped thin film. After introducing Nb into La:$BiFeO_3$, the fatigue resistance is improved. The remanent polarization decreased 23% for the $Bi_{0.9}La_{0.1}Nb_{0.01}Fe_{0.99}O_3$ film in comparison to the 37% decrease for the $Bi_{0.9}La_{0.1}FeO_3$ film after 10^7 read and/or write switching cycles. A similar improvement was also observed after Nb doping into 20% La doped $BiFeO_3$ thin film. The fatigue in perovskite oxides is mainly due to the diffusion and relocation of the oxygen vacancies and electronic-charge trapping at the domain wall during the electrical switching. The reduction in the movable charge density through doping is the direct reason for the improved fatigue resistance. It also proves that Nb doping is more effective than La doping in reducing the charge density.

Measurements of the magnetic hysteresis loops of the pure and doped $BiFeO_3$ thin film samples at room temperature show strong diamagnetic signals, which is because of the dominant amount of substrate in the samples (not shown here). However, the magnetic field cooled and zero field cooled magnetization measurements clearly show that these thin films have magnetic moment at room temperature. To confirm that the ferromagnetism is not canceled due to doping with Nb, the magnetic hysteresis loops of the target bulks were measured. Results show that the doping with Nb and La enhanced the magnetic moment in the bulk. This result is consistent with the observed enhancement of magnetic moment in La doped $BiFeO_3$ ceramics.[11,16]

We report the significant improvement of the ferroelectric properties of $BiFeO_3$ thin film through control of electrical leakage by Nb doping. A very large remanent electrical polarization value of 80 $\mu C/cm^2$ was observed in $Bi_{0.8}La_{0.2}Nb_{0.01}Fe_{0.99}O_3$ thin film on $Pt/Ti/SiO_2/Si$ substrate. The doping effect of Nb in reducing the movable charge density due to oxygen vacancies in $BiFeO_3$ was confirmed by the dielectric measurements. A very small loss was observed in the Nb and La codoped $BiFeO_3$ thin film. As well as the ferroelectric performance improvement from Nb and La codoping, the La doping also enhances the magnetic moment. It is expected that the solution to the problem of control of electrical leakage, which has been a severe obstacle restricting practical application, will open the door to real devices based on $BiFeO_3$ thin films.

The authors would like to thank the Australian Research Council (ARC) for support through Discovery projects (DP0558753 and DP0665873).

[1] B. Ramesh and N. A. Spaldin, Nat. Mater. **6**, 21 (2007).
[2] M. Fiebig, J. Phys. D **38**, R123 (2005).
[3] J. Dho, X. Qi, H. Kim, J. L. MacManus-Driscoll, and M. G. Blamire, Adv. Mater. (Weinheim, Ger.) **18**, 1445 (2006).
[4] Z. X. Cheng, X. L. Wang, C. V. Kannan, K. Ozawa, H. Kimura, T. Nishida, S. J. Zhang, and T. R. Shrout, Appl. Phys. Lett. **88**, 132909 (2006).
[5] J. Wang, J. B. Neaton, H. Zheng, V. Nagarajan, S. B. Ogale, B. Liu, D. Viehland, V. Vaithyanathan, D. G. Schlom, M. Wuttig, and R. Ramesh, Science **299**, 1719 (2003).
[6] T. Zhao, A. Scholl, F. Zavaliche, K. Lee, M. Barry, A. Doran, M. P. Cruz, Y. H. Chu, C. Ederer, N. A. Spaldin, R. R. Das, D. M. Kim, S. H. Baek, B. Eom, and R. Ramesh, Nat. Mater. **5**, 823 (2006).
[7] F. Zavaliche, R. R. Das, D. M. Kim, C. B. Eom, S. Y. Yang, P. Shafer, and R. Ramesh, Appl. Phys. Lett. **87**, 182912 (2005).
[8] F. Bai, J. L. Wang, M. Wuttig, J. F. Li, N. G. Wang, A. P. Pyatakov, A. K. Zvezdin, L. E. Cross, and D. Viehland, Appl. Phys. Lett. **86**, 032511 (2005).
[9] W. Eerenstein, F. D. Morrison, J. Dho, M. G. Blamire, J. F. Scott, and N. D. Mathur, Science **307**, 1203a (2005).
[10] X. D. Qi, J. Dho, R. Tomov, M. Blamire, and J. L. Macmanus-Driscoll, Appl. Phys. Lett. **86**, 062903 (2005).
[11] Y. H. Lin, Q. H. Jiang, Y. Wang, C. W. Nan, L. Chen, and J. Yu, Appl. Phys. Lett. **90**, 172507 (2007).
[12] Z. X. Cheng and X. L. Wang, Phys. Rev. B **75**, 172406 (2007).
[13] K. Y. Yun, D. Ricinschi, T. Kanashima, and M. Okuyama, Appl. Phys. Lett. **89**, 192902 (2006).
[14] C. Lee and J. Wu, Appl. Phys. Lett. **91**, 102906 (2007).
[15] D. Lee, M. G. Kim, S. Ryu, H. M. Jang, and S. G. Lee, Appl. Phys. Lett. **86**, 222903 (2005).
[16] Z. X. Cheng, A. H. Li, X. L. Wang, H. Kimura, K. Ozawa, and S. X. Dou, J. Appl. Phys. (to be published April 2008).
[17] D. Lebeugle, D. Colson, A. Forget, and M. Viret, Appl. Phys. Lett. **91**, 022907 (2007).